On Holmboe's instability for smooth shear and density profiles

Alexandros Alexakis
National Center for Atmospheric Research, Boulder, Colorado 80305

(Received 21 January 2005; accepted 22 June 2005; published online 2 August 2005)

The linear stability of a stratified shear flow for smooth density profiles is studied. This work focuses on the nature of the stability boundaries of flows in which both Kelvin–Helmholtz and Holmboe instabilities are present. For a fixed Richardson number the unstable modes are confined to finite bands between a smallest and a largest marginally unstable wavenumber. The results in this paper indicate that the stability boundary for small wavenumbers is comprised of neutral modes with phase velocity equal to the maximum/minimum wind velocity whereas the other stability boundary, for large wavenumbers, is comprised of singular neutral modes with phase velocity in the range of the velocity shear. We show how these stability boundaries can be evaluated without solving for the growth rate over the entire parameter space as was previously done. The results indicate further that there is a new instability domain that has not been previously noted in the literature. The unstable modes, in this new instability domain, appear for larger values of the Richardson number and are related to the higher harmonics of the internal gravity wave spectrum. © *2005 American Institute of Physics*. [DOI: 10.1063/1.2001567]

I. INTRODUCTION

Stratified shear flow instabilities occur in a variety of physical contexts such as astrophysics,[1] the Earth's atmosphere and oceanography.[2–5] The linear instability problem of stratified shear flows has been addressed in a large body of literature. Since the original work of Helmholtz[6] and Lord Kelvin[7] many models of flows and density stratifications have been investigated both analytically and numerically. Parametrized by the global Richardson number, these investigations have resulted in a large variety of stability/instability domains in the Richardson number–wavenumber space.[8–11] However, a full understanding of this large variety of stability domains does not exist.

A step toward understanding a particular aspect of shear flow instability was achieved by Holmboe.[12] Using a piecewise-linear form of the velocity and density profile Holmboe managed to distinguish between two classes of unstable modes that are present in stratified shear flows. In the first class the unstable modes have zero phase velocity in a reference frame of zero-mean velocity and exist for a finite range of strength of the stratification (Richardson number). This instability is referred to in the literature as Kelvin–Helmholtz instability since the behavior of the unstable modes resembles the one predicted by Kelvin–Helmholtz. The unstable modes of the second class have nonzero phase velocity and typically smaller growth rate than the Kelvin–Helmholtz modes. However, they are present for arbitrarily large values of strength of the stratification, making them better candidates to explain certain physical phenomena. This second kind of instability is referred to as Holmboe instability.

Several authors have expanded Holmboe's work[13–15] by considering different stratification and velocity profiles that do not include the simplifying symmetries Holmboe used in his model. Discussions on the mechanisms involved in the instability can be found in Refs. 13 and 16. Hazel[17] and more recently Smyth and Peltier[18] have shown that Holmboe's results hold for smooth density and velocity profiles as long as the length scale of the density variation is sufficiently smaller than the length scale of the velocity variation. Further, effects of viscosity and diffusivity,[19] nonlinear evolution[20–22] and mixing properties[23] of the Holmboe instability have also been investigated. Experimentally, Holmboe's instability has been investigated by various groups. Browand and Winant[24] first performed shear flow experiments in stratified environments under the conditions that Holmboe's instabilities are present. Their investigation has been extended further by more recent experiments.[15,25–29] The unstable Holmboe modes have been observed and Holmboe's predictions verified.

In this work we examine the stability of smoothly stratified shear flows as was done in Refs. 17 and 18, but here we focus on finding the kind of marginally unstable modes that comprise the stability boundaries. We show how these modes can be determined without solving the full eigenvalue problem for the complex eigenvalue c. Furthermore, our results indicate that new instability regions exist which have not been discovered before in the literature.

This paper is structured as follows. In Sec. II we formulate the linear stability problem and discuss the possible marginally unstable modes that can comprise the stability boundaries. In Sec. III we describe the numerical methods used. Section IV presents our results. Specifically, we show the location of the marginally unstable modes and numerically verify that they indeed constitute the stability boundaries. Conclusions are drawn in Sec. V where we also give a physical description of our results.

II. FORMULATION

We begin with the Taylor–Goldstein equation, which describes linear normal modes of a parallel shear flow in a stratified, inviscid, nondiffusive, Boussinesq fluid:

$$\phi'' - \left[k^2 + \frac{U''}{U-c} - \frac{J(y)}{(U-c)^2} \right] \phi = 0, \tag{1}$$

where $\phi(y)$ is the complex amplitude of the stream function for a normal mode with real wavenumber k and complex phase velocity c. $\mathrm{Im}\{c\}>0$ implies instability with growth rate given by $\gamma = k\,\mathrm{Im}\{c\}$. $U(y)$ is the unperturbed velocity in the x direction and $J(y) = -g\rho^{-1} d\rho/dy$ is the squared Brunt–Väisäla frequency. Prime indicates differentiation with respect to y. We note that when c is real and in the range of U there is a height y_c, at which $U(y_c)=c$. At the height y_c, called the critical height, Eq. (1) has a regular singular point. Many of the features of the unstable modes are related to the presence of this singular point. Equation (1) together with the boundary conditions $\phi \to 0$ for $y \to \pm\infty$, forms an eigenvalue problem for the complex eigenvalue c.

The Taylor–Goldstein equation (1), has been studied for many different density and velocity profiles and is known to have four different classes of modes as solutions:[30] (i) For some conditions unstable modes exist with the real part of the phase velocity within the range of U. The phase speed of these modes satisfies Howard's semicircle theorem $|c - 1/2(\sup\{U\}+\inf\{U\})| < 1/2|\sup\{U\}-\inf\{U\}|$. Furthermore, if these modes exist the Miles–Howard theorem[31] guarantees that somewhere in the flow the local Richardson number defined by

$$\mathrm{Ri}(y) = \frac{J(y)}{[U'(y)]^2} \tag{2}$$

must be smaller than $1/4$. As discussed in the Introduction, for some velocity and density profiles, the class of the unstable modes can be further divided into two subclasses of unstable modes, those whose phase velocity is zero with respect the mean flow (Kelvin–Helmholtz modes) and those whose phase velocity is nonzero, the Holmboe modes. (ii) The complex conjugates of the unstable modes constitute the second class of modes. That is, for each (c_u, ϕ_u) that is a solution of (1) that describes an unstable mode there is a solution (c_d, ϕ_d) that describes a damped mode with $c_d = c_u^*$ and $\phi_d = \phi_u^*$. (iii) The third class of modes consists of nonsingular traveling modes with phase velocity outside the range of U. These are internal gravity wave modes modified by the shear. (iv) Finally, due to the singularity at the critical height y_c a continuum of singular neutral modes exist with a singular behavior of the first derivative of the steam function at the critical height. The phase velocity of these modes lies within the range of U. For these modes an asymptotic analysis close to the critical height shows that the stream function can be written as the sum of two linearly independent solutions:

$$\phi \simeq A^{\pm}(|y-y_c|^{s_a} + \cdots) + B^{\pm}(|y-y_c|^{s_b} + \cdots), \tag{3}$$

where $s_a = 1/2 - \sqrt{1/4 - \mathrm{Ri}(y_c)}$, $s_b = 1/2 + \sqrt{1/4 - \mathrm{Ri}(y_c)}$ and the index $\pm$ corresponds to the solution above or below the critical height. The solutions in Eq. (3) are known as the Frobenius solutions. If these modes are marginally unstable the Frobenius solutions need to be considered as the limit $\mathrm{Im}\{c\} \to 0^+$ and yield the connection formulas:

$$A^- = e^{i s_a \pi} A^+ \text{ and } B^- = e^{i s_b \pi} B^+. \tag{4}$$

For each wavenumber and fixed density and velocity profiles more than one of the above-mentioned modes can exist. Consequently, it is interesting to try and find boundaries, if they exist, that separate these four classes of modes. This is what we try to achieve in what follows for a specific example of shear and stratification.

The example we investigate follows Hazel's[17] work where the velocity profile is given by

$$U(y) = \tanh(y). \tag{5}$$

Note that the problem has been is nondimensionalized using the half-thickness and the half-velocity change of the shear layer. For the stratification as, in Ref. 17, we pick the squared Brunt–Väisäla frequency's functional form (in nondimensional units) to be given by

$$J(y) = J_0\,\mathrm{sech}^2(Ry), \tag{6}$$

where R^{-1} gives the nondimensional length scale of the density stratification. The symmetry $J(y)=J(-y)$ and $U(y)=-U(-y)$ implies that if $[c, \phi(y)]$ is the eigenvalue and eigenfunction of an unstable mode, then $[-c^*, \phi(-y)]$ is also a solution of Eq. (1) that describes an unstable mode traveling in the opposite direction. This allows us with no loss of generality to focus only on the modes that have $Re\{c\}>0$.

The following observations illuminate the origin and possible location of the stability boundaries. First, as noted by Hazel,[17] for the density and velocity profile given in Eqs. (6) and (5), respectively, the functional form of the local Richardson number crucially depends on the value of the parameter R (see Fig. 1). For $R \leqslant \sqrt{2}$, the local Richardson number has a unique minimum at $y=0$ given by $\mathrm{Ri}(0)=J_0$. This implies that we can only have instability if $J_0 < 1/4$ (Ref. 31) and any stability boundary must lie within this region or on its boundary. For $\sqrt{2} < R < 2$ two minima exist symmetrically around zero and therefore we can have instability for values of J_0 larger than $1/4$. For $R=2$, $\mathrm{Ri}(y)$ obtains its minimum value for $y=\pm\infty$ with $\mathrm{Ri}(\pm\infty)=1/4J_0$ and therefore instability can occur only if $J_0<1$. Finally for

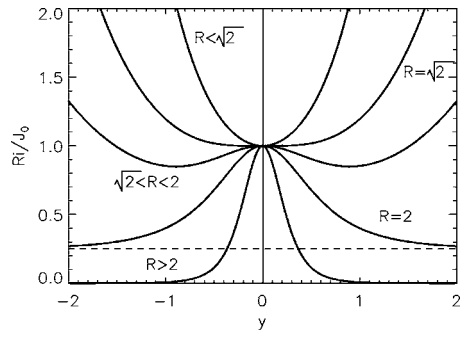

FIG. 1. The local Richardson number $Ri(y)$ normalized by J_0 for different values of the parameter R.

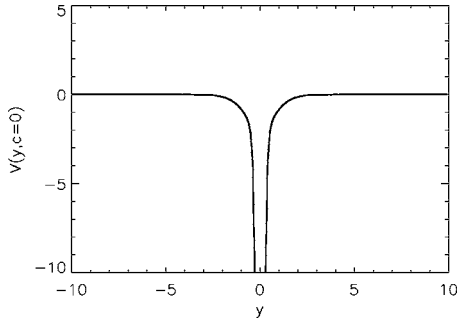

FIG. 2. The potential $V(y,c)$ in Eq. (7) for $c=0$.

larger values of R, Ri(y) decays exponentially to zero as y becomes large and an instability might be present at arbitrarily large values of J_0.

In order to make the second observation we need to transform Eq. (1) into an alternative form. Denoting $E=-k^2$ and $V(y,c)=U''/(U-c)-J/(U-c)^2$ we can rewrite the Taylor–Goldstein equation as

$$\phi'' = [V(y,c) - E]\phi. \tag{7}$$

Now, if we invert the problem and ask the question, for a given real phase velocity c what is the value of $k^2=-E$ that satisfies the above equation and boundary conditions, we end up with a Schrödinger problem for a particle in a potential well given by $V(y,c)$. Figure 2 shows the resulting singular potential for $c=0$, $R=1$ and $J_0=2$. The solution of this particular problem for $R=1$ gives the stability boundary for the unstable modes given by the relation $J_0=k(1-k)$ as shown in Ref. 32. Figure 3 shows the resulting potential for $c=1$ and three values of $R=1,2,4$. If $R<2$ no solution exists that satisfies the boundary conditions since this problem corresponds to finding bounded states in an unbounded potential well $[V(y,1)\to-\infty$ for $y\to+\infty]$. However, if $R\geqslant 2$ we have to solve for the eigenstates/energy levels of a particle in a finite potential well. For this case a discrete number of bounded energy states with "energy levels" E_n exist. Each state corresponds to a mode with $c=1$ and wavenumber $k_n=\sqrt{-E_n}$. Since the phase speed of free gravity waves is a decreasing function of wavenumber, we expect that wavenumbers smaller than $\sqrt{-E_n}$ will have $|c|<1$ and could possibly be unstable. Of course, whether these solutions indeed represent marginally unstable modes still needs to be demonstrated. Note that marginally unstable modes with phase velocity equal to the maximum velocity of the shear flow have been reported before in the literature in interfacial gravity wave generation problems.[33–35]

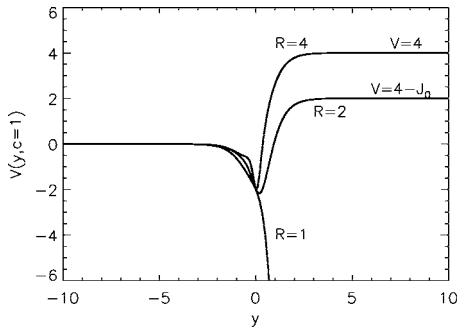

FIG. 3. The potential $V(y,c)$ in (7) for $c=1$ for three different values of R. Only when $R\geqslant 2$ bounded states are allowed.

Besides the modes with $c=1$, other neutral modes that may be marginally unstable should have c in the range of U and therefore must be singular. These modes can be written in terms of the asymptotic expansion in Eq. (3). For example, let $\phi(y)=A^+f_a(y)+B^+f_b(y)$ be the exponentially decaying solution of of the Taylor–Goldstein equation 1 for $y>y_c$ [where f_a and f_b are the two Frobenius solutions in (3)]. A^+ and B^+, with no loss of generality, are assumed real. The connection formulas for marginally unstable modes (3) imply that below the critical layer $(y<y_c)$ the solution will be $\phi(y)=[A^+\cos(s_a\pi)f_a(y)+B^+\cos(s_b\pi)f_b(y)]+i[A^+\sin(s_a\pi)f_a(y)+B^+\sin(s_b\pi)f_b(y)]$. However, only one linear combination of f_a and f_b will give an exponentially decaying solution for $y\to-\infty$. Therefore, if A^+ and B^+ are such that the real part of $\phi(y)$ is decreasing exponentially to zero for $y\to-\infty$ the imaginary part of $\phi(y)$ will increase exponentially. Since both the real and the imaginary parts of ϕ need to satisfy the boundary conditions at infinity it seems unlikely that such a solution exists unless one of the two coefficients A^+ or B^+ is zero. Therefore, a possible marginally unstable mode would be a singular mode that is proportional to only one of the two independent Frobenius solutions in Eq. (3) (i.e., $A^\pm=0$ or $B^\pm=0$). However, the existence of such a solution is not guaranteed, so in addition, a suitable value of k^2 and $c<1$ needs to be found (if it exists) so that both boundary conditions are satisfied. We note that the case in which the $c=0$ modes form a stability boundary corresponds to a special case of this class of marginally unstable modes.

III. NUMERICAL METHODS

The strategy that we adopt in order to find the unstable regions is the following. First we find the location of the neutral modes described in the previous section and then investigate if these modes are indeed marginally unstable by solving for the growth rate (or for Im{c}) in the neighborhood of these modes. Four different numerical codes were used. Each code integrates the Taylor–Goldstein equation (1) using a fourth-order Runge–Kutta method (tested for different resolutions to verify convergence) and a shooting method is used to determine the eigenvalue in the four different eigenvalue problems that we describe in more detail below.[36]

In the first eigenvalue problem we take $c=0$. For a given value of J_0 we integrate the Taylor–Goldstein equation from zero to infinity with initial conditions given by one of the two Frobenius solutions (3), and look for the eigenvalue k^2 such that the boundary condition at infinity is satisfied. Note that for symmetry reasons, when $c=0$, only the positive y-axis needs to be considered. The solution of this problem provides us with the stability boundary for the Kelvin–Helmholtz modes, as shown in Ref. 17. We will refer to this problem as eigenvalue problem one. The values of J_0 that satisfy the condition $c=0$ for a wavenumber k will be denoted by the curve $J_0=J_{KH}(k)$.

For the second eigenvalue problem we take $c=1$ and solve the Schrödinger problem for the potential $V(y,1)$ by integrating Eq. (7) from $-$"∞" to $+$"∞" and look for the eigenvalue E_n for which the boundary condition at $+$"∞" is satisfied (where by "∞" we mean sufficiently large value of y). The modes evaluated from this process are nonsingular neutral modes, and form a curve in the (J_0-k) plane that we denote by $J_0=J_1(k)$.

In the third problem we are looking for the values of c ($c\neq 0$ and $\mathrm{Im}\{c\}=0$) and k such that one of the two independent Frobenius solutions of Eq. (3) satisfies both boundary conditions at infinity. In more detail the third code begins with an initial "guess" of both c and k and integrates from the critical height both forward and backward up to some sufficiently large positive/negative value of y. The initial conditions for ϕ and ϕ' at $y=y_c\pm dy$ (where dy is a small deviation from the critical height) are obtained from Eq. (3) with either $A^{\pm}=0$ or $B^{\pm}=0$ (both cases were tested) and terms up to second order in the expansion are used. As argued in the previous section, only the solution that it is proportional to one of the two linearly independent solutions of (3) can satisfy the connection formulas across the critical layer (for marginally unstable singular modes) and both boundary conditions at infinity. Any other linear combination of the Frobenius solutions (3) will lead to a singular neutral mode that does not belong to an instability boundary. Since we begin with either $A^{\pm}=0$ or $B^{\pm}=0$ we are only left with two conditions to satisfy at $\pm$"∞" and two parameters to change (c and k). With a bisection method[36] the code converged to a single pair of values of c and k. For one of the two initial conditions (say $A^{\pm}=0$) the code converged to the $c=1$ solution, and for the second initial condition (say $B^{\pm}=0$) the code converged to a value of c and k with $-1<c<1$. The solutions with $c\neq 1$ comprise a class of singular neutral modes forming a curve in the (J_0-k) plane that we will denote by $J_0=J_{1S}(k)$.

However, the existence of the above-mentioned neutral modes does not guarantee that they form a stability boundary. Hence, a code that solves the full eigenvalue problem for the complex eigenvalue c was used to verify that the above-mentioned neutral solutions constitute the stability boundaries. This fourth code integrates the Taylor–Goldstein equation from $\pm$"∞" to zero for some given values of J_0 and k and a Newton–Raphson method is used to find the value of c for which the two solutions match at zero. No approximation is used to cross the critical height and for this reason this code converged only for unstable modes ($\mathrm{Im}\{c\}\neq 0$) and neutral nonsingular gravity waves ($|c|>1$). Note that this code encounters problems with convergence when the examined parameters are very close to a neutral singular mode stability boundary because of the almost singular behavior in the neighborhood of the critical height that needs to be resolved.

IV. RESULTS

A. Small values of J_0

We begin with relatively small values of J_0 (order unity or less) which is the case that has been previously examined by Refs. 17 and 18. However, in Refs. 17 and 18 the authors determined the instability boundaries in the (J_0-k) plane by solving the full eigenvalue problem in the examined parameter space, finding in that way the regions with nonzero growth rates. This is a very difficult task since in order to determine the instability region, the entire (J_0-k) plane needs to be mapped for every value of R. Here we use a different approach. We find the location of the neutral modes corresponding to the different eigenvalue problems described in the last section and show that these form instability boundaries by solving the complex value of the phase velocity only for a few values of the global Richardson number.

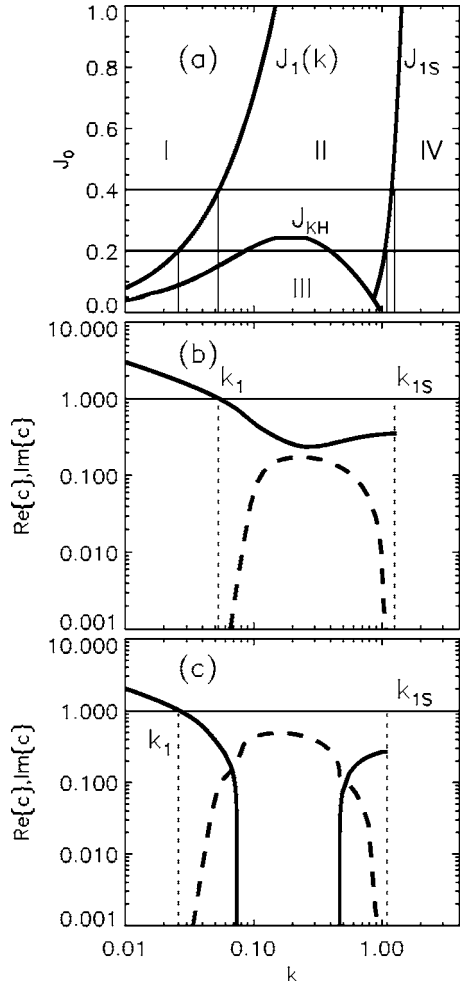

FIG. 4. (a) The stability boundaries for $R=4$. In region (I) stable gravity waves exist with $|c|>1$. In region (II) unstable waves with the real part of the phase velocity in the range $0<|\mathrm{Re}\{c\}|<1$ exist. In region (III) unstable KH modes with $\mathrm{Re}\{c\}=0$ exist. In region (IV) only neutral singular modes exist. The stability boundary $J_1(k)$ is composed of the modes with $c=1$. The stability boundary $J_{KH}(k)$ is composed of the modes with $c=0$. The stability boundary $J_{1S}(k)$ is composed of the singular neutral modes with $c\neq 0$. The horizontal lines correspond to the values of J_0 examined in (b) and (c). (b) The real (solid line) and imaginary (dashed line) phase velocity for $J_0=0.4$. Unstable modes exist for wavenumbers in the range $k_1<k<k_{1S}$. (c) The real (solid line) and imaginary (dashed line) phase velocity for $J_0=0.2$. Unstable modes exist for wavenumbers in the range $k_1<k<k_{1S}$. In both cases $\mathrm{Im}\{c\}$ is approaching zero in the boundaries of the range (k_1,k_{1S}). All panels share a common x-axis.

In Fig. 4 we show the results for the case $R=4$. As was found in previous work[17,18] the (J_0-k) plane can be divided in four regions [see panel (a)]. In the first region (I) free

gravity waves exist with real phase velocity of absolute value greater than one. In the second region (II) unstable Holmboe waves exist with the real part of the phase velocity smaller than one but different from zero. In the third region (III) unstable Kelvin–Helmholtz modes are present with the real part of the phase velocity equal to zero. Finally in the fourth region (IV) only singular neutral modes exist. The three lines that separate these regions were constructed by finding the neutral modes with the properties described in the previous section. In more detail the curve $J_1(k)$ that separates region (I) from region (II) is composed of modes that have phase velocity equal to one ($c=1$). The curve $J_{KH}(k)$ that separates region (II) from region (III) is composed of singular modes with $c=0$. Finally the curve $J_{1S}(k)$ that separates region (II) from region (IV) is composed of singular modes with $c\neq 0$.

Further illumination of how the properties of a mode change as we increase the wavenumber is gained by looking at panels (b) and (c) of Fig. 4 that show the dispersion relation (phase velocity as a function of the wavenumber) for two values of J_0 [panel (b) $J_0=0.4$ and panel (c) $J_0=0.2$]. A logarithmic scale is used to focus on the details of small wavenumbers and small phase velocities. For the $J_0=0.4$ case, for small wavenumbers the phase velocity is real and decreases with k until the phase velocity becomes equal to one ($c=1$ mode) for some wavenumber $k_1\simeq 0.05$ such that $J_1(k_1)=0.4$. For wavenumbers larger than k_1 the phase velocity becomes complex indicating that the mode with $c=1$ belongs to the stability boundary. As we further increase the wavenumber there is a critical value k_{1S} for which the imaginary part of the phase velocity becomes zero again, with the real part of the phase velocity remaining finite and smaller than one. This mode with wavenumber k_{1S} can only be a singular neutral mode and can be represented by the expansion given in Eq. (3) with the connection formulas given in Eq. (4). Indeed the difference between the wavenumber where the imaginary part of c becomes zero (found by the fourth eigenvalue problem) and the wavenumber k_{1S} (found by solving the third eigenvalue problem), is found (for this case and all the cases examined) to be of the order of the numerical error. The small difference is attributed to the difficulty in resolving the almost singular region around y_c with the fourth code when $\mathrm{Im}\{c\}$ is very small.

For smaller values of the global Richardson number $[\mathrm{Ri}(0)=J_0<0.25]$ we have the extra feature that as we approach the stability boundary composed of modes with $c=0$ the real part of the phase velocity decreases to zero. It remains zero in region (III) and then starts to increase again in region (II) until region (IV) is met. We note that in region (IV) a continuum of singular stable modes exist and for this reason we do not plot the phase velocity after this point.

The next question we examine is how the stability boundaries change as we vary the value of the parameter R. In Fig. 5 we plot the stability boundaries for four different values of R [panel (a) $R=4$, panel (b) $R=2.5$, panel (c) $R=2.2$ and panel (d) $R=2$]. For large values of the parameter R ($R>2$) the (J_0-k) plane is divided in four regions determined by the boundaries J_1, J_{1S}, J_{KH} as discussed in more detail in Fig. 4. The wavenumbers k of the Holmboe unstable modes are confined in a finite strip. As we decrease the value

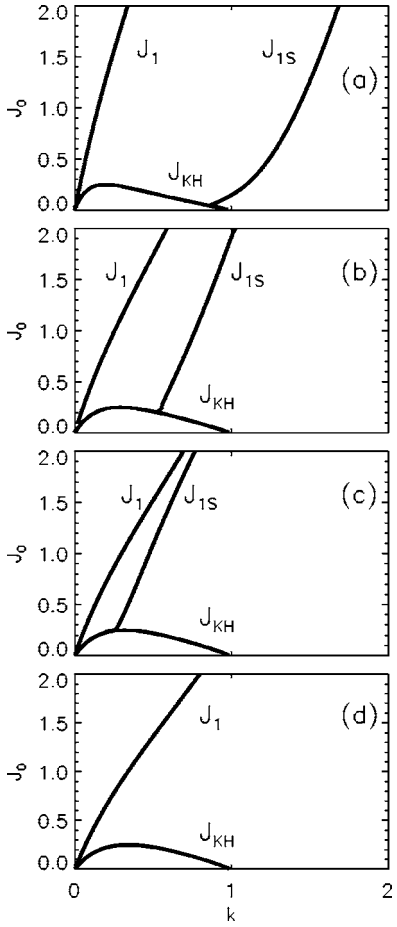

FIG. 5. The dependence of the instability boundaries on the parameter R. The four panels show the stability boundaries for four values of R. (a) $R=4$, (b) $R=2.5$, (c) $R=2.2$, (d) $R=2$. Note that for the last case, $R=2$, in (d) the stability boundary $J_1(k)$ composed of modes with the property $c=1$ and the boundary with singular modes $J_{1S}(k)$ have collapsed together and the resulting boundary now defines the region that nonsingular neutral gravity waves exist. All panels share a common x-axis.

of R the width of the strip with Holmboe unstable wavenumbers becomes smaller [see panels (b) and (c)]. When $R=2$ [panel (d)] the two boundaries J_{1S} and J_{1S} collapse together. In this case J_1, J_{1S} does not provide a stability boundary but continues to separate the region that nonsingular gravity wave modes exist (on the left of J_1) from the region that only singular neutral modes exist with $0<c<1$ (on the right of J_1). The only unstable modes for this case are the Kelvin–Helmholtz modes confined in the finite region in the left bottom corner.

We note here that Ref. 18 did not find Holmboe instability for values of of R smaller than 2.4. This is probably because the width of instability strip becomes very small for values of R smaller than 2.4. Furthermore, close to the stability boundaries the growth rate is very small and as a result it is even harder to find a positive growth rate using the method used in Ref. 18 when the two stability boundaries are too close. To verify that this strip is unstable we plot in Fig. 6 a close up of the instability region and the dispersion relation for $J_0=0.4$ for the case of $R=2.2$.

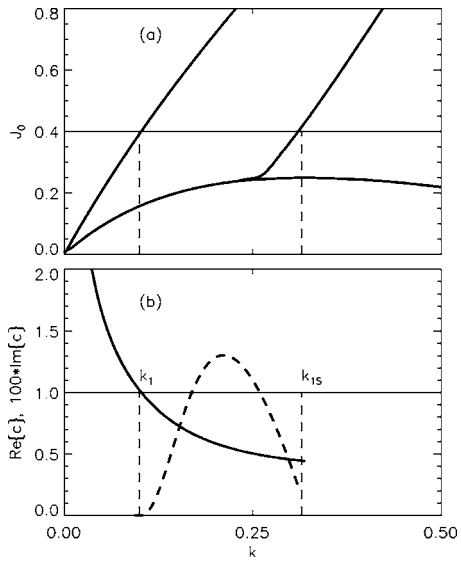

FIG. 6. The stability boundaries (a) and the dispersion relation ($J_0=0.4$) (b) for the case that $R=2.2$. In (b) solid line gives the real part of c and the dashed line gives the imaginary part of c. Unstable Holmboe modes exist for this case also but are confined in a very narrow region.

B. Higher harmonics

As we have shown, finding the modes that satisfy $c=1$ can be reduced to finding the eigenstates of a particle in a finite potential well. It is well known from quantum mechanics that if a potential well is deep enough a finite number $N \geqslant 1$ of bound states will exist with N different energy levels E_n and wavefunctions ϕ_n ($n=1,2,\ldots,N$). If the modes with $c=1$ form one of the stability boundaries for the Holmboe instability, it is natural to ask what happens for the case that J_0 is large enough [i.e., the potential well in the Schrödinger problem (7) is deep enough] so that more than one mode satisfies the condition $c=1$ (i.e., more than one bounded eigenstate is allowed). We note that a discontinuous density profile will lead to a delta-function behavior of $J(y)$ that allows only one eigenstate and for this reason higher harmonic waves are not present in step-function density profiles like the ones examined in Ref. 12.

To investigate the possible existence of higher harmonic unstable modes we solve for the modes with $c=1$ for values of J_0 up to 10^2. We find that the higher harmonics of the gravity waves with $c=1$ indeed exist and correspond to new stability boundaries that we denote as $J_n(k)$. The second harmonic ($n=2$) with $c=1$ appears for $J_0 \simeq 28$ and the third harmonic ($n=3$) for $J_0 \simeq 80$. We also find that for each $c=1$ mode a marginally singular neutral mode with $0<c<1$ also exists. These modes form new curves in the (J_0-k) plane given by $J_{nS}(k)$. These curves $J_n(k)$ and J_{nS}, define new stripes of unstable regions.

In Fig. 7 we plot the stability domain for values of J_0 up 100 for $R=4$. The stable regions are marked with S and the regions that the nth harmonic becomes unstable are marked with U_n. The solid lines show $J_n(k)$ and correspond to modes with $c=1$ and the dashed lines show $J_{nS}(k)$ and correspond to marginally unstable singular modes. As before we verify that unstable modes exist in the regions between $J_n(k)$ and $J_{nS}(k)$

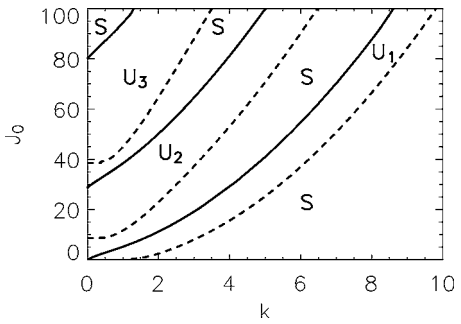

FIG. 7. Instability diagram for larger values of J_0 and $R=4$. Solid lines show $J_n(k)$, dashed lines show $J_{nS}(k)$. The stable regions are marked with S. Regions marked with U_n are regions that the nth harmonic becomes unstable.

by solving for the complex phase velocity of the modes in these regions. In Figs. 8 and 9 [panel (a)] we show a closeup of the stability boundaries $J_2(k), J_{2S}(k)$ and $J_3(k), J_{3S}(k)$, respectively, and the dispersion relation in panel (b). Figures 8 and 9 demonstrate how the second and the third gravity wave harmonic become unstable.

We note finally that for a fixed value of J_0 the highest harmonic has the largest growth rate. In Fig. 10 we show the growth rate $\gamma=k\,\mathrm{Im}\{c\}$ as a function of the wavenumber for $R=4$ and two different values of J_0. The growth rate is significantly larger for the highest harmonic. This makes the higher unstable harmonics possible to be detected experimentally, since it is the most unstable modes that are usually observed.

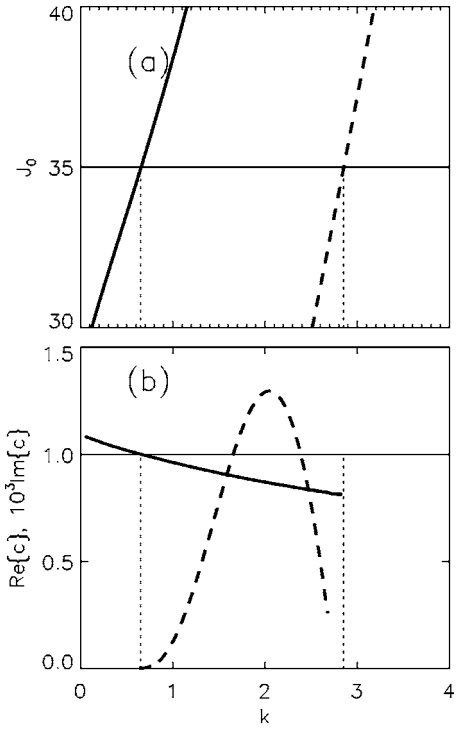

FIG. 8. (a) The stability boundaries for the second harmonic for $R=4$. Solid line gives $J_2(k)$, dashed line gives $J_{2S}(k)$. (b) The real part of the phase velocity (solid line) and the imaginary part of the phase velocity (dashed line) for $J_0=35$.

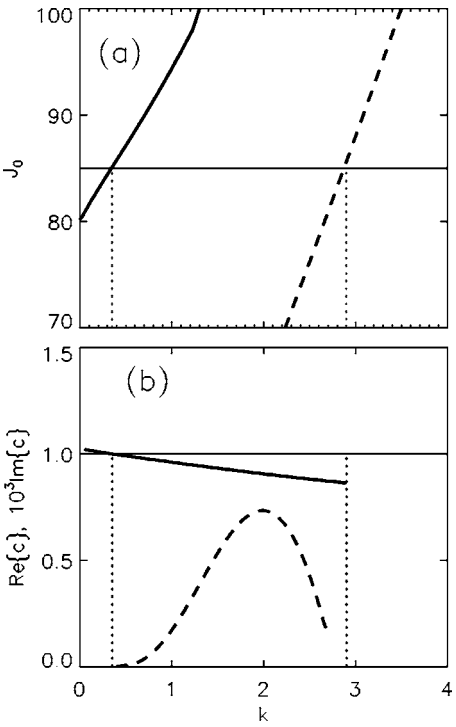

FIG. 9. (a) The stability boundaries for the third harmonic for $R=4$. Solid line shows $J_3(k)$ and dashed line shows $J_{3S}(k)$. (b) The real part of the phase velocity (solid line) and the imaginary part of the phase velocity (dashed line) for $J_0=85$.

V. CONCLUSIONS AND PHYSICAL DESCRIPTION

In this paper we investigated Holmboe's instability in stratified shear flows for smooth density and velocity profiles. Using a specific model of the density and velocity profiles,[17,18] we were able to determine the instability regions for large values of the global Richardson number including regions not previously noted in the literature.

Focusing on the nature of the stability boundaries that enclose the Holmboe unstable modes, we have shown that for moderate values of J_0 and when the density stratification length scale is sufficiently smaller than the shear length scale (i.e., $R>2$) the (J_0-k) plane is divided into four regions: (I) a region where neutral gravity waves exist (i.e., modes with real phase velocity outside the range of the velocity shear); (II) a region where unstable traveling waves exist (i.e., Holmboe modes); (III) a region where unstable modes with the real part of the phase velocity being zero exist (i.e., Kelvin Helmholtz modes); (IV) and finally a region where only singular neutral modes exist. We determined the modes that comprise the boundaries and separate these four classes of modes. For small J_0 $(J_0<1/4)$ Kelvin–Helmholtz modes exist. They are restricted in a bounded domain enclosed by the boundary $J_0=J_{KH}(k)$ determined by the modes with zero phase velocity. For larger J_0, a strip of Holmboe unstable modes exist. This instability strip is determined by the two boundaries $J_0=J_1(k)$ and $J_0=J_{1S}(k)$. In more detail, we have demonstrated that for a given value of the global Richardson number J_0 the unstable modes have wavenumbers k that lie in the range $k_1<k<k_{1S}$ where k_1 is the wavenumber of the mode that has phase velocity equal to one and satisfies $J_0=J_1(k_1)$ and k_{1S} is the wavenumber of a singular marginally unstable neutral mode. k_{1S} satisfies $J_0=J_{1S}(k_{1S})$. We have shown how the value of k_1 and k_{1S} can be determined to desired accuracy (and therefore how to construct the boundaries $J_1(k)$ and $J_{1S}(k)$) by solving a Schrödinger eigenvalue problem for a particle in a potential well.

For large values of the global Richardson number more than one strip of instability may appear. Each new instability strip is confined between the pair of curves $J_0=J_n(k)$ and $J_0=J_{nS}(k)$. As before $J_n(k)$ can be determined for a given value of J_0 by finding the wavenumber k_n of the nth harmonic of the gravity wave spectrum with $c=1$ and $J_{nS}(k)$ is determined by finding the wavenumber k_{nS} of the singular marginally unstable mode that is met first as we increase the wavenumber from k_n.

The results of this paper show a deep connection between the free gravity wave spectrum and the Holmboe unstable waves. The overall picture looks as follows. For large stratification and small wavenumbers the free gravity wave spectrum is only slightly modified by the shear and is composed of a discrete finite number N $(N\geqslant 1)$ of stable modes (ϕ_n, c_n) with $n=1,2,\ldots,N$. As the wave number is increased the phase speed decreases roughly as the square root of the wavenumber. As the phase speed approaches the maximum shear velocity $(\sup\{U\})$, the functional form of the stratification plays a crucial role. If the stratification length scale is larger than a critical value [more precisely if $\lim_{y\to\infty} \mathrm{Ri}(y) \to\infty$] the phase speed approaches $\sup\{U\}$ asymptotically as $k\to\infty$, always remaining outside the range of U. In this case the only unstable wavenumbers are the Kelvin–Helmholtz modes that have zero phase velocity and appear only for a finite range of the global Richardson number. If the stratification length scale is smaller than this critical value [more precisely if $\lim_{y\to\infty} \mathrm{Ri}(y)\to 0$], the phase speed of the waves reaches the value of the maximum wind speed for a finite value of the wavenumber $k=k_n$. As we increase the wavenumber further, the modes become unstable with the real part of the phase velocity smaller than one. The instability persists up to another critical value of the wavenumber $k=k_{nS}$. The mode with this wavenumber exhibits a singular behavior at the critical height. For wavenumbers smaller than k_{nS} a continuum of singular neutral modes exist.

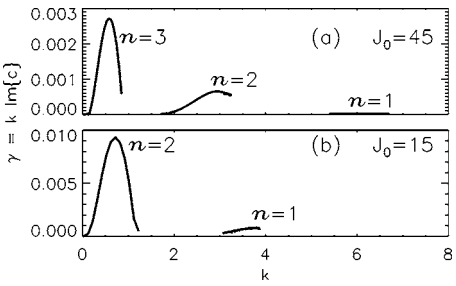

FIG. 10. The growth rate for the different unstable harmonics. (a) $J_0=45$, $R=4$. (b) $J_0=15$, $R=4$. For the smallest harmonics for which the Im$\{c\}$ was very small the code was able to find the growth rate only around the peak and not close to the stability boundaries. For the $J_0=45$ case in (a) the growth rate of the first harmonic $(n=1)$ was too small for the code to be able to resolve the critical height and the dark line just indicates the location of the instability region based on the stability boundaries shown in Fig. 7.

The findings in this work suggest several possibilities for further investigation. An important aspect that needs to be investigated is the effect of viscosity and diffusivity. As the work in Ref. 19 has shown, the presence of finite viscosity and diffusivity decreases the growth rate and this effect is expected to be stronger for the higher harmonics. This may limit attempts to detect the higher harmonic modes via numerical and experimental studies. Therefore, an investigation of the viscosity effects is further needed to find the critical Reynolds number for which the higher modes become unstable and this should be the next step in the study of the higher harmonics instability. Nonetheless, we note that in most astrophysical and geophysical flows, where Holmboe's instability is of great importance, the Reynolds and Peclét numbers are large enough that the inviscid flow examined here is a good approximation, and depending on the stratification the higher harmonic modes might dominate.

Finally, besides viscosity and dissipation, three-dimensional effects, nonlinear evolution and saturation, as well as physical interpretation of these results through simplified layer models are all important issues that we plan to investigate in our future work.

ACKNOWLEDGMENTS

The author acknowledges support from NCAR/GTP. The National Center for Atmospheric Research is supported by the National Science Foundation. The author is grateful to L. Howard for his suggestions and references at the beginning of this work, and would also like to thank K. MacGregor, J. Mason and J. Sukhatme for their comments. Finally, during the review process the comments by W. D. Smyth helped to bring this manuscript to its final form and his help is appreciated.

[1] R. Rosner, A. Alexakis, Y. Young, J. Truran, and W. Hillebrand, "On the C/O enrichment of novae ejecta," Astrophys. J. **562**, L177 (2002).
[2] L. Armi and D. M. Farmer, "The flow of Mediterranean water through the Strait of Gibraltar," Prog. Oceanogr. **21**, 1 (1988).
[3] T. Oguz, E. Ozsoy, M. A. Latif, H. I. Sur, and U. Unluata, "Modeling of hydraulically controlled exchanged flow in the Bosphorous Strait," J. Phys. Oceanogr. **20**, 945 (1990).
[4] F. E. Sargent and G. H. Jirka, "Experiments on saline wedge," J. Hydraul. Eng. **113**, 1307 (1987).
[5] S. Yoshida, M. Ohtani, S. Nishida, and P. F. Linden, "Mixing processes in a highly stratified river," *Physical Processes in Lakes and Oceans*, edited by J. Imberger (American Geophysical Union, Washington, D.C., 1998).
[6] H. Helmholtz, "Ueber discontinuirliche Flüssigkeitsbewegungen," Wissenschaftliche Abhandlungen **3**, 146 (1868).
[7] Lord Kelvin, "Influence of wind and capillarity on waves in water supposed frictionless," in *Mathematical and Physical Papers IV, Hydrodynamics and General Dynamics* (Cambridge University Press, Cambridge, 1910), p. 76.
[8] L. N. Howard, "Neutral curves and stability boundaries in stratified shear flow," J. Fluid Mech. **16**, 333 (1963).
[9] L. N. Howard and P. G. Drazin, "Hydrodynamic stability of parallel flow of inviscid fluid," Adv. Appl. Mech. **9**, 1 (1966).
[10] L. N. Howard and S. A. Maslowe, "Stability of stratified shear flows," Boundary-Layer Meteorol. **4**, 511 (1973).
[11] P. G. Drazin and W. H. Reid, *Hydrodynamic Stability* (Cambridge University Press, Cambridge, 1981).
[12] J. Holmboe, "On the behavior of symmetric waves in stratified shear layers," Geophys. Publ. **24**, 67 (1962).
[13] C. P. Caulfield, "Multiple linear instability of layered stratified shear flow," J. Fluid Mech. **258**, 255 (1994).
[14] S. P. Haigh and G. A. Lawrence, "Symmetric and non-symmetric Holmboe instabilities in an inviscid flow," Phys. Fluids **11**, 1459 (1999).
[15] G. A. Lawrence, F. K. Browand, and L. G. Redecopp, "The stability of a sheared density interface," Phys. Fluids A **3**, 2360 (1991).
[16] P. G. Baines and H. Mitsudera, "On the mechanism of shear flow instabilities," J. Fluid Mech. **276**, 327 (1994).
[17] S. P. Hazel, "Numerical studies of the stability of inviscid shear flows," J. Fluid Mech. **51**, 3261 (1972).
[18] W. D. Smyth and W. R. Peltier, "The transition between Kelvin–Helmholtz and Holmboe instability; An investigation of the over-reflection hypothesis," J. Atmos. Sci. **46**, 3698 (1989).
[19] W. D. Smyth and W. R. Peltier, "Three-dimensional primary instabilities of a stratified dissipative, parallel flow," Geophys. Astrophys. Fluid Dyn. **52**, 249 (1990).
[20] W. D. Smyth, G. P. Klaasen, and W. R. Peltier, "Finite amplitude Holmboe waves," Geophys. Astrophys. Fluid Dyn. **43**, 181 (1988).
[21] W. D. Smyth and W. R. Peltier, "Instability and transition in in finite amplitude Kelvin–Helmholtz and Holmboe waves," J. Fluid Mech. **228**, 387 (1991).
[22] B. R. Sutherland, C. P. Caulfield, and W. R. Peltier, "Internal gravity generation and hydrodynamic instability," J. Atmos. Sci. **51**, 3261 (1994).
[23] W. D. Smyth and K. B. Winters, "Turbulence and mixing in Holmboe waves," J. Phys. Oceanogr. **33**, 694 (2003).
[24] F. K. Browand and C. D. Winant, "Laboratory observations of shear layer instability in a stratified fluid," Boundary-Layer Meteorol. **5**, 67 (1973).
[25] C. G. Koop, "Instability and turbulence in a stratified shear layer," Tech. Rep. USCAE 134, Department of Aerospace Engineering, University of South California (1976).
[26] O. Pouliquen, J. M. Chomaz, and P. Huerre, "Propagating Holmboe waves at the interface between two immiscible fluids," J. Fluid Mech. **266**, 277 (1994).
[27] D. Z. Zhu and G. A. Lawrence, "Holmboe's instability in exchange flows," J. Fluid Mech. **429**, 391 (2001).
[28] A. M. Hogg and G. N. Ivey, "The Kelvin–Helmholtz to Holmboe instability transition in stratified exchange flows," J. Fluid Mech. **477**, 339 (2003).
[29] N. Yonemitsu, G. E. Swaters, N. Rajaratnam, and G. A. Lawrence, "Shear instabilities in arrested salt wedge flows," Dyn. Atmos. Oceans **24**, 173 (1996).
[30] W. H. H. Banks, P. G. Drazin, and M. B. Zaturska, "On the normal modes of parallel flow of inviscid stratified fluid," J. Fluid Mech. **75**, 149 (1976).
[31] L. N. Howard, "A note on a paper of John Miles," J. Fluid Mech. **10**, 509 (1961).
[32] J. Miles, "On the stability of heterogeneous shear flow Part 2," J. Fluid Mech. **16**, 209 (1963).
[33] A. Alexakis, Y. Young, and R. Rosner, "Shear instability of fluid interfaces: A linear analysis," Phys. Rev. E **65**, 26313 (2002).
[34] A. Alexakis, Y. Young, and R. Rosner, "Weakly non-linear analysis of wind driven gravity waves," J. Fluid Mech. **505**, 171 (2004).
[35] S. M. Churilov, "Stability analysis of stratified shear flows with a monotonic velocity profile without inflection points," Izv. Akad. Nauk, Fiz. Atmos. Okeana **40**, 725 (2004).
[36] W. H. Press, B. P. Flannery, S. A. Teukolosky, and W. T. Vetterling, *Numerical Recipes* (Cambridge University Press, Cambridge, 1987).